Citation: Clinical and Translational Gastroenterology (2016) 7, e138; doi:10.1038/ctg.2015.66
© 2016 the American College of Gastroenterology All rights reserved 2155-384X/16
www.nature.com/ctg

# Alcoholic Liver Disease: A Mouse Model Reveals Protection by *Lactobacillus fermentum*

Rosario Barone, PhD[1,2,8], Francesca Rappa, PhD[1,2,3,8], Filippo Macaluso, PhD[1,2], Celeste Caruso Bavisotto, PhD[1,2], Claudia Sangiorgi, PhD[1], Gaia Di Paola, BSc[1], Giovanni Tomasello, MD[1,2], Valentina Di Felice, PhD[1,2], Vito Marcianò, BSc[4], Felicia Farina, MD[1], Giovanni Zummo, MD[1], Everly Conway de Macario, PhD[5], Alberto J.L. Macario, MD[2,5], Massimo Cocchi, MD[6,7], Francesco Cappello, MD[1,2] and Antonella Marino Gammazza, PhD[1,2]

**Objectives: Alcoholism is one of the most devastating diseases with high incidence, but knowledge of its pathology and treatment is still plagued with gaps mostly because of the inherent limitations of research with patients. We developed an animal model for studying liver histopathology, Hsp (heat-shock protein)-chaperones involvement, and response to treatment.**

**Methods: The system was standardized using mice to which ethanol was orally administered alone or in combination with *Lactobacillus fermentum* following a precise schedule over time and applying, at predetermined intervals, a battery of techniques (histology, immunohistochemistry, western blotting, real-time PCR, immunoprecipitation, 3-nitrotyrosine labeling) to assess liver pathology (e.g., steatosis, fibrosis), and Hsp60 and iNOS (inducible form of nitric oxide synthase) gene expression and protein levels, and post-translational modifications.**

**Results: Typical ethanol-induced liver pathology occurred and the effect of the probiotic could be reliably monitored. Steatosis score, iNOS levels, and nitrated proteins (e.g., Hsp60) decreased after probiotic intake.**

**Conclusions: We describe a mouse model useful for studying liver disease induced by chronic ethanol intake and for testing pertinent therapeutic agents, e.g., probiotics. We tested *L. fermentum*, which reduced considerably ethanol-induced tissue damage and deleterious post-translational modifications of the chaperone Hsp60. The model is available to test other agents and probiotics with therapeutic potential in alcoholic liver disease.**

*Clinical and Translational Gastroenterology* (2016) **7,** e138; doi:10.1038/ctg.2015.66; published online 21 January 2016
**Subject Category:** Liver

## INTRODUCTION

Alcoholic liver disease (ALD) is caused by alcohol abuse and occurs after years of excessive drinking. The pathogenesis is characterized by progressive accumulation of lipids in the liver (early steatosis), inflammation, steatohepatitis, and in some individuals, the final stages include fibrosis and cirrhosis.[1,2] Induction of oxidative and nitrosative stresses and activation of the inflammatory cascade are implicated in the pathophysiology of ALD.[3,4] Oxidative stress includes cell and tissue damages resulting from an imbalance between excessive production of reactive oxygen species (ROS) and/or reactive nitrogen species (RNS) and limited antioxidant defenses. Mitochondria are the principal source of free radicals and oxidative stress because of inefficiencies in the electron flow along the electron transport chain.[5,6] The liver is one of the richest organs in mitochondria and, in hepatocytes, ROS may have a role in nitric oxide (NO) synthesis and metabolism, caspase activity, and DNA fragmentation.[7] NO acts as a messenger that modulates several cellular processes and is described as a highly toxic and reactive molecule. Conversely, it has also been demonstrated that NO is antiapoptotic in hepatocytes and is required for normal liver regeneration.[8,9] NO is enzymatically synthesized through NO synthase (NOS) and liver contains diverse forms of NOS such as the neuronal form (nNOS, NOS1) in the peribiliary plexus; the inducible form (iNOS, NOS2) in hepatocytes, cholangiocytes, and Kupffer and stelate cells; and endothelial form (eNOS, NOS3) in the endothelial cells.[7] NO easily reacts with the superoxide anion, producing the highly reactive peroxynitrite, and this can produce novel products such as nitrotyrosine (NT), nitrotryptophan, and nitrated lipids that serve as important biological markers *in vivo*.[10] Evaluation of NT levels, along with those of NO, serves to monitor cell damage, as well as the degree of inflammation in diseases associated with oxidative stress.[11]

Among the mediators of stress responses are heat-shock proteins (Hsps), which are induced in the brain and liver by acute and chronic alcohol administration.[4,12] Hsps, many of which are molecular chaperones, are ubiquitous and highly conserved proteins constitutively expressed under normal

[1]Department of Experimental Biomedicine and Clinical Neurosciences, Human Anatomy Section, University of Palermo, Palermo, Italy; [2]Euro-Mediterranean Institute of Science and Technology, Palermo, Italy; [3]Department of Legal Science, Society and Sports, University of Palermo, Palermo, Italy; [4]Department of Microbiology, Parasitology and Virology, Azienda Ospedaliera Universitaria (AOUP), University of Palermo, Palermo, Italy; [5]Department of Microbiology and Immunology, School of Medicine, University of Maryland at Baltimore; and IMET, Baltimore, Maryland, USA; [6]Institute Paolo Sotgiu Quantitative and Evolutionary Psychiatry and Cardiology, L.U.De.S. University, Lugano, Switzerland and [7]Department of Medical Veterinary Sciences, University of Bologna, Bologna, Italy
Correspondence: Antonella Marino Gammazza, PhD, Department of Experimental Biomedicine and Clinical Neurosciences, Human Anatomy Section, University of Palermo, Via del Vespro 129, 90127 Palermo, Italy; E-mail: antonella.marino@hotmail.it
[8]These authors contributed equally to this work.
Received 22 July 2015; accepted 4 Decemeber 2015

temperature with indispensable functions in the life cycle of proteins and with a role in protecting cells from deleterious stressors. Molecular chaperones inhibit aggregation of partially denatured proteins and refold them to maintain protein homeostasis and tissue physiology.[13,14] One member of the Hsps is Hsp60, a molecular chaperone that assists protein folding in mitochondria together with its cochaperone Hsp10.[15] Hsp60 is constitutively expressed under normal conditions and induced by different types of stressors such as, e.g., oxidative stress.[16,17] In the liver, Hsp60 is involved in hepatocellular carcinoma, chronic active hepatitis, and primary biliary cirrhosis.[14] Hsp60 has been considered a major defence system against cellular damage after ethanol administration in the liver and pancreas.[18]

The oxidative stress associated with ALD seems to be caused not only by an increase in pro-oxidants but also via an alteration in the oxidant–antioxidant tissue profile because of poor nutrition or malabsorption in the gastrointestinal tract of the alcoholics.[19,20] The use of dietary supplements reduces body fat mass and lowers cancer risk.[21,22] Probiotics are living microorganisms, usually bacteria that confer numerous beneficial effects on the host's health. *Lactobacillus* and *Bifidobacterium* are the most common types of microbes used as probiotics, but strains of *Bacillus*, *Pediococcus*, and some yeast have also been found as suitable candidates. These microorganisms are part of the normal intestinal microbial flora and are ingested with fermented food with added active live cultures, e.g., yogurt, and other dietary supplements.[23] Encouraging results have been reported on the use of probiotics in the treatment of various disorders such as pouchitis,[24] ulcerative colitis,[25,26] and Crohn's disease.[27] Other studies have shown hypolipidemic and antioxidant properties of a probiotic mixture in hyperlipidemic hamsters.[28] There is evidence for the roles played by commensal bacteria in alcohol-induced liver injury through dysbiosis of the intestinal microbial ecosystem caused by alcohol intake.[29]

Despite the importance of alcoholism and its devastating personal and social impact, with disastrous economic consequences, and despite the great number of studies carried out to understand its pathophysiology and to develop effective therapies, there are still many aspects of this disease that are incompletely understood. One reason for this knowledge gap is that the clinicopathological research and trials of novel therapeutic agents with human patients are extremely limited. It is therefore cogent to develop animal models amenable to histopathological and molecular studies focused on the organs most affected by the disease, for instance, the liver and brain, and that would allow trials of potentially curative agents. In this work, we have standardized a model system using mice, and have focused on the liver and the molecular chaperone Hsp60. In addition, we have tested the effects of a probiotic, *Lactobacillus fermentum*, on the alterations we found in the mice fed with ethanol in their diet.

## METHODS

**The model system: animals and diets.** All animal experiments were approved by the ethics committee for animal experiments at the University of Palermo and adhered to the recommendations in the guide for the care and use of laboratory animals set by the National Institutes of Health (NIH, Bethesda, MD). Moreover, all experiments were performed in the Human Physiology Laboratory of the Department of Experimental Biomedicine and Clinical Neuroscience at the University of Palermo, which was formally authorized by the Ministero della Sanità (Rome, Italy).

The study reported here to standardize and calibrate the mouse model was performed with female 12-month-old mice (BALB/cAnNHsd) obtained from Harlan laboratories S.r.l. (Udine, Italy) (Table 1). The animals were kept at a constant 12 : 12 h light–dark cycle and had free access to food (4RF21 standard diet, Mucedola; Settimo Milanese, Milan, Italy) and water, which was the diet for the control (Con) mice ($n=13$). For the experimental mice, ethanol 96% (EtOH) (Girolamo Luxardo, Torrella, Padova, Italy) was added to account for 15% of total calories. To allow for acclimation to the alcohol diet, the animals were given 5% EtOH-calorie content for 2 days, which was increased to 10% EtOH-calorie content for 2 days, followed by 15% EtOH-calorie content diet[30,31] for 4 (mouse group 4EtOH, $n=5$), 8 (mouse group 8EtOH, $n=5$), and 12 (mouse group 12EtOH, $n=5$) weeks. A calculation to increase the standard caloric need of the mice (14 kcal per day, 3.6 g of their food) with the addition of EtOH was made considering the caloric content of EtOH diluting it in water in a final volume of 100 µl. This volume was orally administered to the mice every day using a pipette. Three additional mouse groups were added: 4EtOH-P (ethanol and probiotic diet), 8EtOH-P, and 12EtOH-P ($n=5$ per group). These mice were given EtOH as the others (groups 4EtOH, 8EtOH, and 12EtOH), but they also received orally, using a pipette, *L. fermentum* probiotic (Bromatech S.r.l., Milan, Italy), $10^9$ CFU (colony-forming unit) per animal in water, each day during the week, with two days off on weekends, until the end of the experiment. The probiotic was given 20 min after the EtOH administration to investigate its efficacy to counteract the deleterious effects of ethanol on the liver. One more group received the ethanol-containing diet for 8 weeks and then the probiotic for 4 weeks (group 8EtOH-4P, $n=5$), as a pilot study to investigate the curative effects of the probiotic on the liver steatosis and oxidative stress induced by the preceding ethanol consumption. Food and water intake were measured every day, and body weight was measured three times weekly. The diet was controlled weighing the food to adjust it to the daily caloric needs of the mice. Mice were killed 48 h following the last treatment.

**Histopathology.** Liver tissue from the same hepatic lobe of all mice was excised from EtOH, EtOH-P, and Con mice, fixed in 10% buffered formalin, and embedded in paraffin as described previously.[32] Thin sections, obtained from paraffin blocks, were stained with hematoxylin–eosin for histological evaluation of liver injury and Masson's trichrome stain was performed for evaluation of liver fibrosis.[33] Slides were examined, and images captured under bright field with a Leica DM5000 upright microscope (Leica Microsystems, Heidelberg, Germany). Liver sections were examined by two expert pathologists in a blind manner, using coded slides and not knowing their source. The mean of the results was used as data. Liver steatosis was classified using a semiquantitative scoring system divided into three fat

**Table 1** Mouse model for EtOH-induced liver disease and testing therapeutic agents, such as probiotics

| Mice[a] | Para[b] | Mouse group | | | | | | | Disease indicators | Materials and methods |
|---|---|---|---|---|---|---|---|---|---|---|
| | | Con[c] | 4EtOH[d] | 8EtOH | 12EtOH | 4EtOH-P | 8EtOH-P | 12EtOH-P | 8EtOH-4P | |
| BALB/cAnNHsd; female; 12 months age; light–dark cycle 12–12 h; 23 °C; 4RF21 standard diet (Mucedola, Italy) | Food and water weight; body weight; caloric intake | | +15% EtOH 4 weeks | +15% EtOH 8 weeks | +15% EtOH 12 weeks | +15% EtOH 4 weeks | +15% EtOH 8 weeks | +15% EtOH 12 weeks | +15% EtOH 8 weeks | Liver steatosis, fibrosis; iNOS levels, Hsp60 levels and gene expression, Hsp60 nitration | Liver tissue; histopathology, immunohistochemistry, qRT-PCR, western blotting, immunoprecipitation, statistical analysis |
| | | | | | | +*L.f.*[e] $10^9$ CFU | +*L.f.* $10^9$ CFU | +*L.f.* $10^9$ CFU | +*L.f.* $10^9$ CFU 4 weeks | | |

Abbreviations: CFU, colony-forming units; EtOH, ethanol; Hsp, heat-shock protein; iNOS, inducible form of nitric oxide synthase; *L.f.*, *Lactobacillus fermentum*; qRT-PCR, real-time quantitative PCR.
[a]Mice characteristics, environmental conditions, and basic diet.
[b]Parameters measured initially and periodically thereafter (see text).
[c]Control group receiving the standard diet only (no ethanol or probiotic).
[d]For the experimental mice, EtOH was added to account for 15% of total calories in the diet. To acclimate the mice to the alcohol-containing diet, they were given 5% EtOH-calorie content for 2 days, then 10% EtOH-calorie content for 2 days, and lastly 15% EtOH-calorie content for 4, 8, and 12 weeks (mouse groups 4EtOH, 8EtOH, and 12EtOH, respectively). In addition, groups 4EtOH-P, 8EtOH-P, and 12EtOH-P received orally the probiotic *L.f.*, $10^9$ CFU per animal per day, 5 days per week until the end of the experiments. Group 8EtOH-4P received the ethanol-containing diet for 8 weeks as group 8EtOH, and then *L.f.*, $10^9$ CFU per animal per day, 5 days per week for 4 weeks. The pertinent EtOH dose was diluted in water to a final volume of 100 µl. This volume was orally administered to the mice every day using a pipette and a tip and, after 20 min, the mice were fed with the probiotic in the same manner.
[e]*L.f.*, a probiotic used to test the suitability of the model to detect effects, beneficial or otherwise, on the disease indicators. These groups can be used as positive controls and as the baseline for comparing efficacy when testing other probiotics or drugs.

grades (grade I = 5–33%; grade II = 34–66%; and grade III = 67–100%).[34]

**Analysis of serum.** The animals were killed by decapitation for blood collection. The serum was separated by centrifugation with 3000 *g* at 4 °C for 10 min and then stored at – 20 °C. Serum aspartate transaminase (AST) and alanine transaminase (ALT) were measured by clinical laboratories of the University of Palermo using an *in vitro* test (Modular Analytics; Roche, Vienna, Austria) for the quantitative determination of the two enzymes in serum on Roche automated clinical chemistry analyzer (Roche/Hitachi Modular; Roche).

**Real-time quantitative PCR.** The quantitative real time PCR (qRT-PCR) technique was performed as described previously.[35,36] Briefly, total RNA was isolated from 300 mg of the liver from Con and experimental mice using TRIzol REAGENT (Sigma-Aldrich, Milan, Italy), according to the manufacturer's instructions. RNA (50 ng) was retrotranscribed using the ImProm-II Reverse Transcriptase Kit (Promega, Milan, Italy) to obtain cDNA, which was amplified using the StepOnePlus Real-Time PCR System (Life Technologies, Monza, Italy). Quantitative Real-Time PCR (qRT-PCR) was performed using GoTaq qPCR Master Mix (A6001; Promega). The mRNA levels were normalized to the levels obtained for hypoxanthine phosphoribosyltransferase 1, for β-glucuronidase, and for glyceraldehyde-3-phosphate dehydrogenase. The cDNA was amplified using the primers indicated in Supplementary Table S1 online and the Rotor-gene 6000 Real-Time PCR Machine (Qiagen GmbH, Hilden, Germany). Changes in the transcript level were calculated using the $2^{-\Delta\Delta CT}$ method.[37]

**Western blotting.** Western blotting was performed as described previously.[38] Equal amounts of protein (40 µg) were separated on sodium dodecyl sulfate-polyacrylamide gel electrophoresis and transferred onto a nitrocellulose membrane (BioRad, Segrate, Italy). After blocking with 5% bovine serum albumin (Sigma-Aldrich), membranes were probed with primary antibodies as follows: mouse anti-Hsp60 monoclonal antibody, LK1 clone (Sigma-Aldrich), dilution 1 : 1000; rabbit polyclonal to iNOS (GeneTex, Irvine, CA), dilution 1 : 2000; mouse anti-β-actin monoclonal antibody (Sigma-Aldrich) diluted at 1 : 1000; by overnight incubation at 4 °C. Protein bands were visualized using the enhanced chemiluminescence detection system (GE Healthcare Life Sciences, Milan, Italy), and the data were evaluated and quantified using the ImageJ Free software (NIH). Each experiment was performed at least three times.

**Immunoprecipitation.** To detect Hsp60 protein nitration, immunoprecipitation was performed. Briefly, equal amounts of protein (500 µg) from total liver tissue lysates from each mouse group (experimental and Con) were incubated with the primary antibody (mouse monoclonal anti-Hsp60, Clone LK1; Sigma-Aldrich) overnight at 4 °C with gentle rotation. Antibody–protein complexes were then immunoprecipitated with antibodies linked to Sepharose G beads (GE Healthcare, Milano, Italy). Nonspecifically bound proteins were removed

by repeated washings with isotonic lysis buffer. Immunoprecipitated proteins were resolved by 10% sodium dodecyl sulfate-polyacrylamide gel electrophoresis and revealed using anti-3-NT primary antibodies (mouse monoclonal to 3-NT; Abcam, San Francisco, CA; dilution 1 : 1400). Each experiment was performed at least three times.

**Immunohistochemistry.** Immunohistochemistry was performed as described previously.[39] Liver sections (5 μm) were mounted on glass slides and deparaffinized. Sections were immersed in 0.3% $H_2O_2$ for 5 min to quench endogenous peroxidase activity, and treated with 10 mM, pH 6.0, 0.05% Tween-20 tri-sodium citrate at 75 °C for 8 min for antigen retrieval. Subsequently, immunohistochemistry was performed using the Histostain-Pluss IHC detection Kit (Histostain-plus Kit3rd Gen IHC Detection Kit; Life Technologies, Monza, Italy) and primary antibodies against the inducible form of NOS (iNOS) (rabbit polyclonal to iNOS, GeneTex; dilution 1 : 200); 3-NT (mouse monoclonal to 3-NT; Abcam; dilution 1 : 200); and Hsp60 (mouse monoclonal antibody, LK1 clone; Sigma-Aldrich). Nuclear counterstaining was carried out using hematoxylin (Dako, Carpinteria, CA). The immunostained tissue sections were examined at x400 and analyzed in a blind manner, using coded slides and not knowing their source. Data from each tissue section (10 fields per section) were pooled to determine mean values, as described previously.[40]

**Statistical analysis.** Statistical analyses were performed using the package GraphPad Prism 4.0 software (GraphPad Prism Software, San Diego, CA). The data obtained for body weight, food and water intake within the groups were compared by one-way analysis of variance for repeated measurements, whereas all the other data were analyzed between the groups (Con vs. all; 4EtOH vs. 4EtOH-P, 8EtOH, and 12EtOH; 8EtOH vs. 8EtOH-P, 12EtOH; 12EtOH vs. 12EtOH-P and 8EtOH-4P) via one-way analysis of variance. If a significant difference was detected by the analysis of variance analyses, this was further evaluated by Bonferroni *post hoc* test. The data were expressed as means ± s.d. The statistical significance threshold was fixed at the level of $P<0.05$.

## RESULTS

**Effects of ethanol consumption and *L. fermentum* administration on hepatic steatosis.** The data obtained for body weight, food and water intake did not show significant differences within and between the groups (Supplementary Tables S2, S3, and S4 online). Liver sections, stained with hematoxylin–eosin and Masson's trichrome, were observed with an optical microscope, for histological evaluation of ALD. For this evaluation, we considered four histological features: steatosis, inflammation, hepatocellular injury, and fibrosis. As seen in the photomicrographs presented in Figure 1a, there was no apparent evidence of inflammation or necrosis in the EtOH-fed mice compared with the Con mice. The stain revealed a temporal increase in hepatic steatosis in EtOH-fed mice compared with Con mice. The hematoxylin- and eosin-stained liver sections showed well-defined vacuolated areas in the hepatocytes in 8EtOH and 12EtOH mice, persisting also after 8EtOH-4P. In the 8EtOH and 12EtOH groups, steatosis of grade II and grade III, respectively, was present, whereas in the 4EtOH mice no sign of liver steatosis was observed. *L. fermentum* administration 20 min after EtOH consumption reduced liver steatosis. Liver sections from the 8EtOH-P and 12EtOH-P groups showed liver steatosis of grade I, whereas the 8EtOH-4P group showed a liver steatosis of grade II, namely lower degrees of steatosis compared with the matched groups not receiving the probiotic. The liver steatosis score increased significantly in 8EtOH and 12EtOH-fed mice compared with the Con and 4EtOH ($P<0.001$); the score was also significantly higher in 12EtOH compared with 8EtOH-fed mice ($P<0.001$) (Figure 1b, EtOH groups). In EtOH-P groups, liver steatosis score increased significantly in 8EtOH-P and 12EtOH-P mice compared with the Con and 4EtOH-P ($P<0.001$); the score was also significantly higher in 12EtOH-P compared with 8EtOH-P ($P<0.001$) and in 8EtOH-4P compared with Con and 12EtOH-P ($P<0.001$) (Figure 1b, EtOH-P groups). Liver steatosis decreased significantly in 8EtOH-P compared with 8EtOH ($P<0.001$), as well as in 12EtOH-P and 8EtOH-4P compared with 12EtOH ($P<0.001$) (Figure 1b, EtOH/EtOH-P groups). The trichrome stain showed the absence of fibrosis in all specimens (see Supplementary Figure S1 online). Collagen was present only in the portal space and, in limited amounts, in perisinusoidal (Disse) spaces of the lobule in all liver samples.

**Effects of *L. fermentum* administration on AST and ALT levels.** The degree of liver injury by the alcohol was evaluated by measuring the content of liver enzymes AST and ALT in the serum (Figure 2a). The serum AST levels (Figure 2a) were significantly increased in 12EtOH compared with the Con, 4EtOH, 8EtOH, 12EtOH-P, and 8EtOH-4P groups ($P<0.001$). The histogram also shows an increase of AST levels in 12EtOH-P compared with the Con, 4EtOH-P, and 8EtOH-P fed groups. A significant increase was also apparent in 8EtOH-4P compared with the Con group (Figure 2a). The ALT levels (Figure 2b) significantly increased in all the groups compared with the Con group and in 12EtOH compared with 4EtOH and 8EtOH ($P<0.05$). Moreover, there was an increase of the enzyme levels in 8EtOH-4P compared with 12EtOH-P ($P<0.001$).

**Effects of ethanol consumption and *L. fermentum* administration on iNOS and 3-NT levels.** NO-derived pro-oxidants iNOS protein expression was evaluated as a marker of hepatic dysfunction and cytotoxicity because of chronic exposure to EtOH. As shown in Figure 3a, the *iNOS* gene expression levels did not change in the EtOH/EtOH-P groups as compared with the control group. Western blotting showed that EtOH consumption increased the levels of iNOS protein after 8 and 12 weeks compared with control and 4EtOH mice (Figure 3b,c $P<0.01$). iNOS levels decreased significantly in 12EtOH-P and in 8EtOH-4P compared with 12EtOH-fed group (Figure 3b,c) ($P<0.01$). iNOS immunoreactivity was detected in control liver sections, confirming

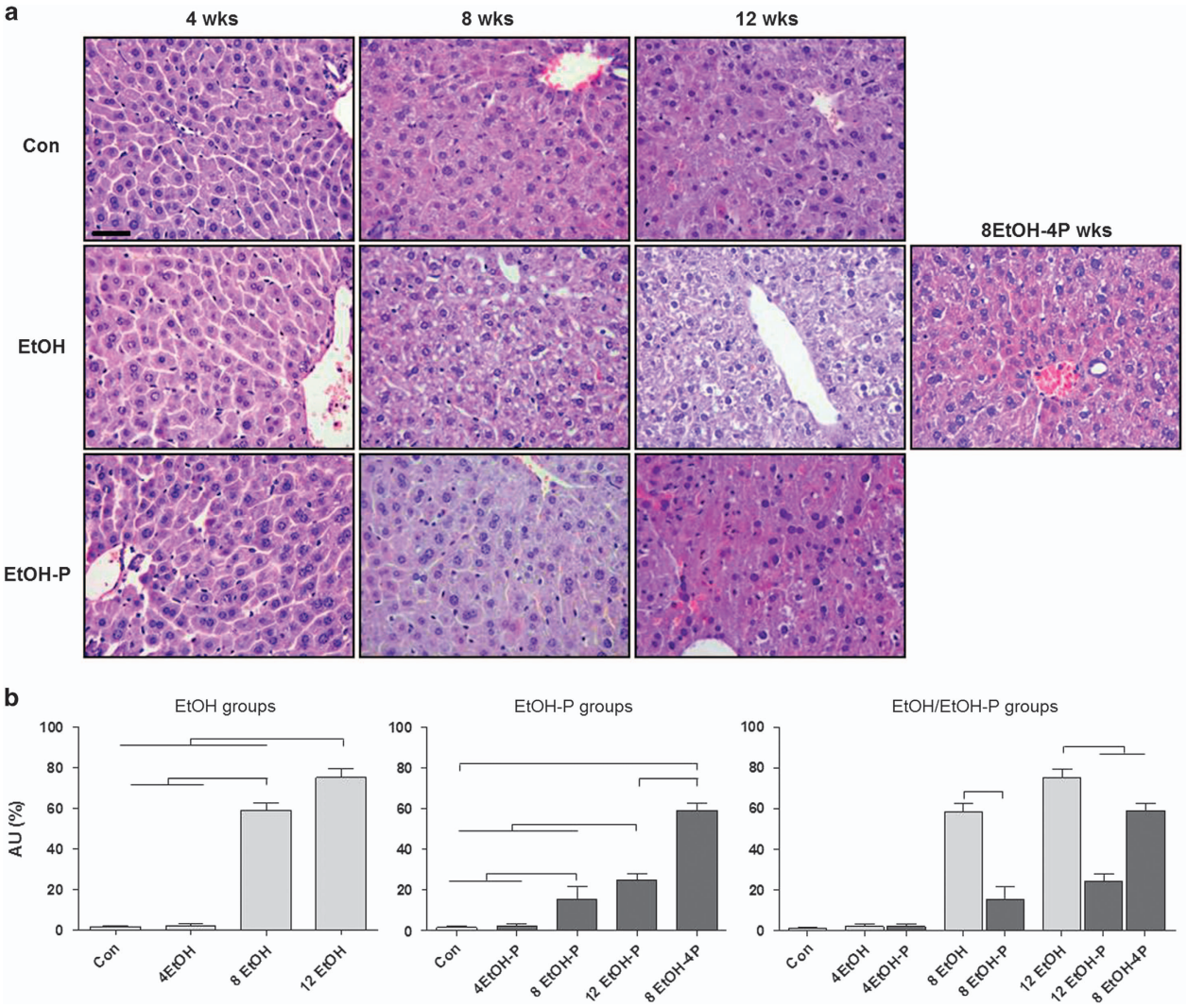


**Figure 1** Representative photomicrographs of liver sections stained with hematoxylin–eosin. (**a**) Liver histology of mice fed control (Con), ethanol (EtOH) diets, and ethanol and probiotic diet (EtOH-P). Bar = 100 μm for all panels. (**b**) Histogram representing the degree of hepatic steatosis as determined by severity scores from I to III. The score is represented as percentage of steatosis (grade I = 5–33%; grade II = 34–66%; grade III = 67–100%). Results are expressed as mean ± s.d. In **b**, the horizontal lines on top of the histograms indicate a significant difference within the groups ($P<0.001$). For further explanation of abbreviations and model features see Table 1. AU, arbitrary unit; 4EtOH, ethanol-fed mice for 4 weeks; 8EtOH, ethanol-fed mice for 8 weeks; 12EtOH, ethanol-fed mice for 12 weeks; 4EtOH-P, ethanol and probiotic-fed mice for 4 weeks; 8EtOH-P, ethanol and probiotic-fed mice for 8 weeks; 12EtOH-P, ethanol and probiotic-fed mice for 12 weeks; 8EtOH-4P, ethanol-fed mice for 8 weeks and then given probiotic for 4 weeks; wks, weeks.

that the protein was constitutively present in hepatocytes (Figure 4a). Cellular localization for iNOS was both cytoplasmic and nuclear in sections derived from the liver of EtOH-fed mice. Tissue levels of iNOS increased in all treated mice groups compared with the Con group, and the increase was statistically significant ($P<0.001$) (Figure 4b). iNOS immunoreactivity decreased in 4EtOH-P compared with 4EtOH ($P<0.01$) and in 8EtOH-4P compared with 12EtOH ($P<0.001$).

Hepatic nitrosative stress was evaluated by immunohistochemical staining of 3-NT indicating peroxynitrite-dependent nitration of protein tyrosine residues. As shown in Figure 5a, 3-NT immunoreactivity increased in the EtOH-fed groups and its distribution was both cytoplasmic and nuclear. The semiquantitative analysis revealed that the increase was statistically significant for all treated animal groups compared with the Con group ($P<0.001$) (Figure 5b). The histogram shows a significant decrease of 3-NT immunoreactivity in 8EtOH-P compared with 4EtOH-P, 8EtOH, or 12EtOH-P ($P<0.001$). A significant increase was also registered in 12EtOH compared with 8EtOH and 8EtOH-4P ($P<0.05$).

**Effects of ethanol consumption and *L. fermentum* administration on *hsp60* gene expression and protein levels.** As EtOH consumption causes mitochondrial dysfunction and protein nitration in the liver, *hsp60* gene expression, Hsp60 protein levels, and tissue distribution were evaluated using qRT-PCR, western blotting, and immunohistochemistry. As shown in Figure 6a, expression of the *hsp60*

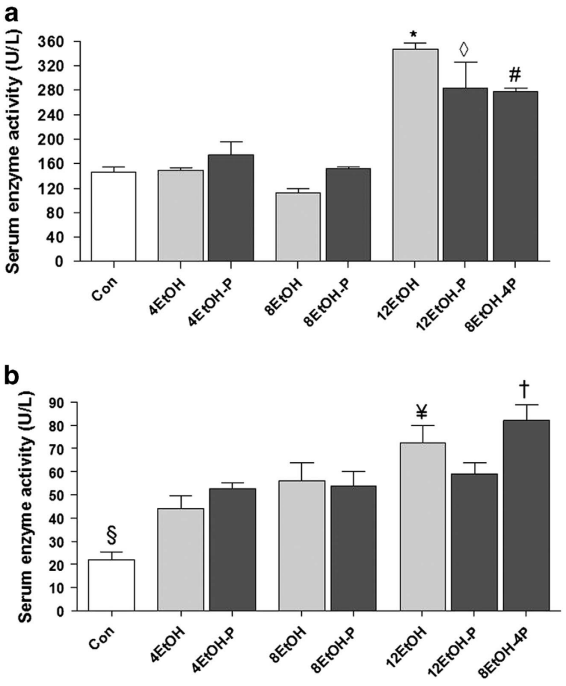


**Figure 2** Aspartate transaminase (AST) and alanine transaminase (ALT) levels in the serum of mice. Histograms showing (**a**) AST and (**b**) ALT levels. Each value is expressed as mean ± s.d. $^{*}P<0.001$ vs. Con, 4EtOH, 8EtOH, 12EtOH-P, and 8EtOH-4P; $^{\lozenge}P<0.001$ vs. Con, 4EtOH-P, and 8EtOH-P; $^{\#}P<0.001$ vs. Con; $^{\S}P<0.001$ vs. all other groups; $^{¥}P<0.05$ vs. 4EtOH and 8EtOH; $^{+}P<0.001$ vs. 12EtOH-P. For the meaning of the abbreviations in **a** and **b**, indicating each mouse group, see legend for Figure 1 and Table 1. Con, control; 4EtOH, ethanol-fed mice for 4 weeks; 8EtOH, ethanol-fed mice for 8 weeks; 12EtOH, ethanol-fed mice for 12 weeks; 4EtOH-P, ethanol and probiotic-fed mice for 4 weeks; 8EtOH-P, ethanol and probiotic-fed mice for 8 weeks; 12EtOH-P, ethanol and probiotic-fed mice for 12 weeks; 8EtOH-4P, ethanol-fed mice for 8 weeks and then given probiotic for 4 weeks.

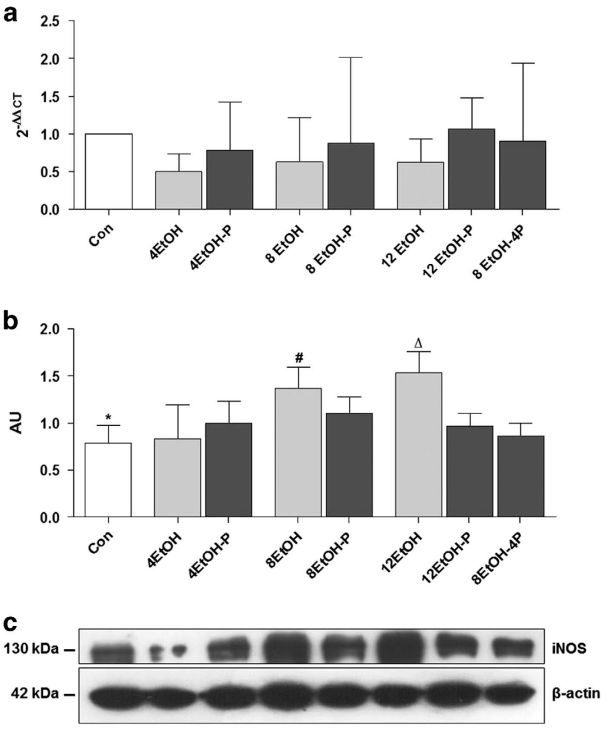


**Figure 3** Inducible form of NOS (iNOS) levels in the liver of control (Con) and ethanol (EtOH) fed mice. (**a**) The bars indicate the degree of the *iNOS* gene expression normalized for the reference genes, according to the Livak method ($2^{-\Delta\Delta CT}$), in the liver of control (Con), ethanol diets, and ethanol and probiotic diet mice. (**b**) Ratio iNOS levels/β-actin levels as a reflection of iNOS increase and decrease (mean ± s.d.). One-way analysis of variance, Bonferroni *post hoc* test. (**c**) Representative cropped blots for iNOS in Con and EtOH-fed mice. The gels were run under the same experimental conditions and β-actin was used as an internal control. $^{*}P<0.01$ vs. 8EtOH and 12EtOH; $^{\#}P<0.01$ vs. 4EtOH; $^{\Delta}P<0.01$ vs. 4EtOH, 12EtOH-P, and 8EtOH-4P. For the meaning of the abbreviations in **a** and **b**, indicating each mouse group, see legend for Figure 1 and Table 1. AU, arbitrary unit; Con, control; 4EtOH, ethanol-fed mice for 4 weeks; 8EtOH, ethanol-fed mice for 8 weeks; 12EtOH, ethanol-fed mice for 12 weeks; 4EtOH-P, ethanol and probiotic-fed mice for 4 weeks; 8EtOH-P, ethanol and probiotic-fed mice for 8 weeks; 12EtOH-P, ethanol and probiotic-fed mice for 12 weeks; 8EtOH-4P, ethanol-fed mice for 8 weeks and then given probiotic for 4 weeks.

gene in the liver was upregulated in 4EtOH-P- and 8EtOH-fed mice compared with the control group ($P<0.01$), and in 4EtOH-P compared with 12EtOH-P ($P<0.05$). Western blotting analysis showed that the Hsp60 protein levels significantly increased in the 8EtOH group as compared with the Con and 4EtOH groups, and in the 8EtOH-P group compared with Con and to 4EtOH-P groups ($P<0.05$; Figure 6b,c). Immunohistochemical staining for Hsp60 revealed that there were low levels of the chaperonin protein in hepatocytes from control mice and, in contrast, these levels increased with the increase in alcohol consumption (Figure 7a). Conversely, high Hsp60 levels were present in the 8EtOH-P mice, but the proteins level decreased after 12 weeks of alcohol consumption alone or in combination with the probiotic (Figure 7a). The semiquantitative analysis showed that Hsp60 levels in the liver tissue significantly increased in all treated mice groups (except for 4EtOH) compared with the Con group. Hsp60 immunoreactivity also increased significantly in 12EtOH compared with 4EtOH ($P<0.01$) (Figure 7b). Similarly, the increase of the protein levels was significant in 8EtOH-P compared with 4EtOH-P and 12EtOH-P ($P<0.05$).

Double-labeled immunoprecipitation of 3-NT and the chaperonin revealed that the quantity of nitrated Hsp60 significantly increased in 12EtOH-fed mice compared with 8EtOH but in contrast nitrated Hsp60 decreased in 12EtOH-P compared with 12EtOH (Figure 8).

## DISCUSSION

Many studies have attempted to identify the molecular pathways affected directly or indirectly by alcohol in the liver. These pathways range from oxidative stress, metabolism-related phenomena, and inflammation to apoptosis. Key events for the onset and progression of ALD result, in part, from gut–liver interaction.[29,41] Consumption of large quantities of alcoholic beverages leads to disturbances in the intestinal absorption of sodium, water, and nutrients, which contributes to the tendency in alcoholics to develop diarrhea. Furthermore, alcohol abuse can result in duodenal erosions, bleeding and mucosal injury in the upper jejunum.[42] Commensal bacteria have a fundamental role in alcohol-induced liver

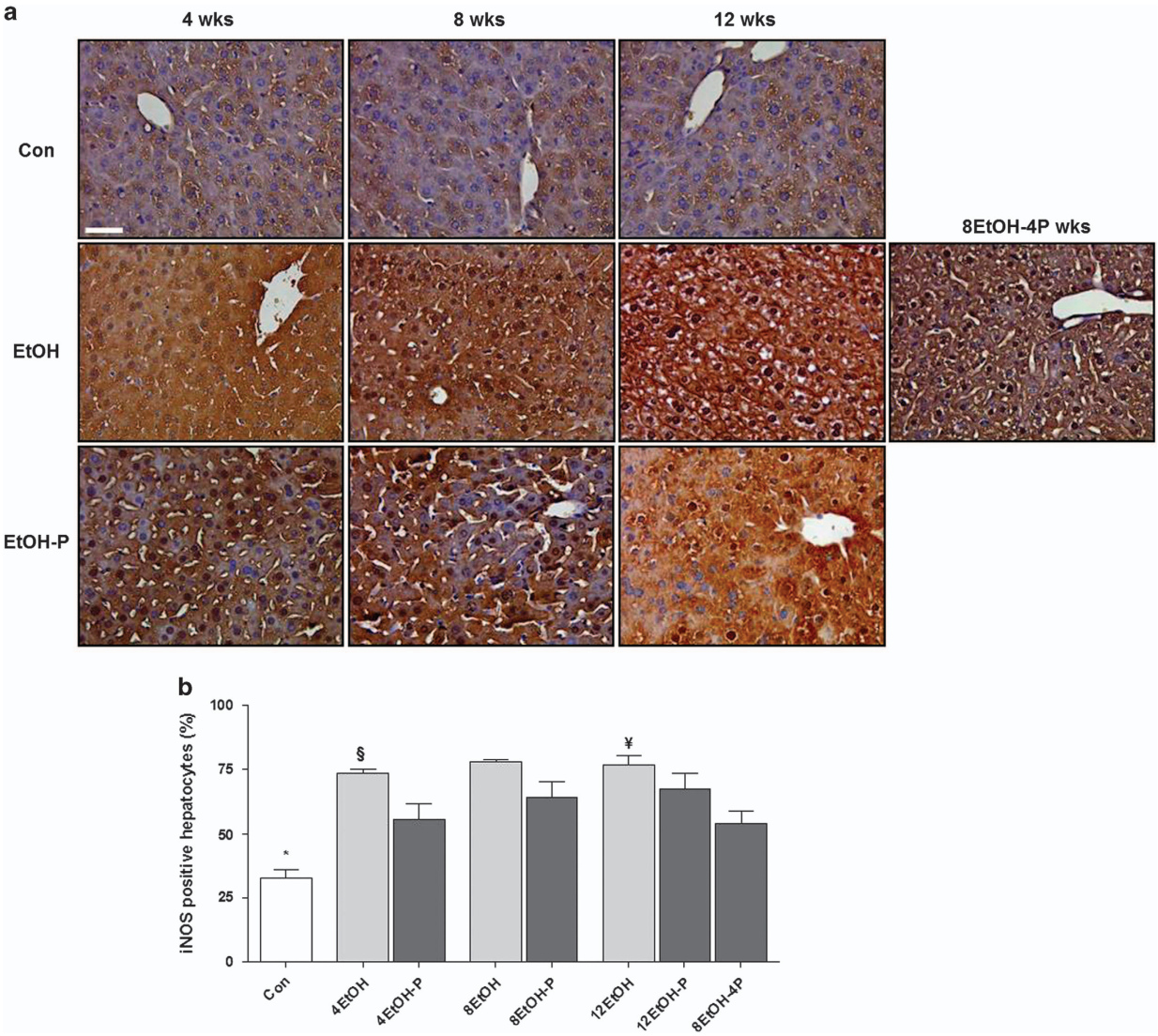


**Figure 4** Hepatocellular distribution of the inducible form of NOS (iNOS). (**a**) Representative photomicrographs of liver sections immunohistochemically stained for iNOS showing iNOS distribution both in the nucleus and the cytoplasm of hepatocytes. Strong staining for iNOS was present in the liver cells after 4, 8, and 12 weeks of alcohol intake, but when alcohol intake was accompanied with the probiotic, the staining intensity decreased. Bar = 100 μm for all panels. (**b**) Histogram showing the percentages of hepatocytes positive for iNOS. The analysis was conducted in a blind manner (using coded slides with the observer not knowing the source of them) and the results are expressed as mean ± s.d. $^{*}P < 0.001$ vs. all other groups; $^{\S}P < 0.01$ vs. 4EtOH-P; $^{¥}P < 0.001$ vs. 8EtOH-4P. For the meaning of the abbreviations in **a** and **b**, indicating each mouse group, see legend for Figure 1 and Table 1. Con, control; 4EtOH, ethanol-fed mice for 4 weeks; 8EtOH, ethanol-fed mice for 8 weeks; 12EtOH, ethanol-fed mice for 12 weeks; 4EtOH-P, ethanol and probiotic-fed mice for 4 weeks; 8EtOH-P, ethanol and probiotic-fed mice for 8 weeks; 12EtOH-P, ethanol and probiotic-fed mice for 12 weeks; 8EtOH-4P, ethanol-fed mice for 8 weeks and then given probiotic for 4 weeks; wks, weeks.

injury through the shift of the composition of the gut microbiota (dysbiosis) caused by alcohol intake.[29] The gut is a habitat for billions of microorganisms and the gut mucosal epithelium serves as a barrier between microbiota and gut tissue.[43] Alcohol abuse not only causes gut leakiness but also affects the composition of colonic mucosa-associated bacterial microbiota in alcohol-fed rats.[44] Moreover, there is evidence of Gram-negative bacterial overgrowth in the gut of alcoholics.[42] Alcohol or its metabolites, e.g. acetaldehyde,[45] disrupt the intestinal barrier and increase gut permeability by various mechanisms such as increased ROS[46] and iNOS[47] and alteration of microRNAs.[48] The disruption of the intestinal barrier causes bacterial and endotoxins translocation in the portal circulation, leading to liver dysfunction, inflammation, fibrosis, and steatosis.[41] It is, therefore, reasonable to hypothesize that the restoration of normal intestinal flora may be of help in the treatment of ALD. In this regard, animal experiments have demonstrated that attenuation of ethanol-induced intestinal permeability, endotoxemia, and liver injury can be achieved using antibiotics, dietary supplements, and probiotics.[49] However, it is necessary to point out that the microbiota in mice is different from that of humans; nonetheless, mice have become the model of choice and a powerful tool for most studies in the emerging field of human gut

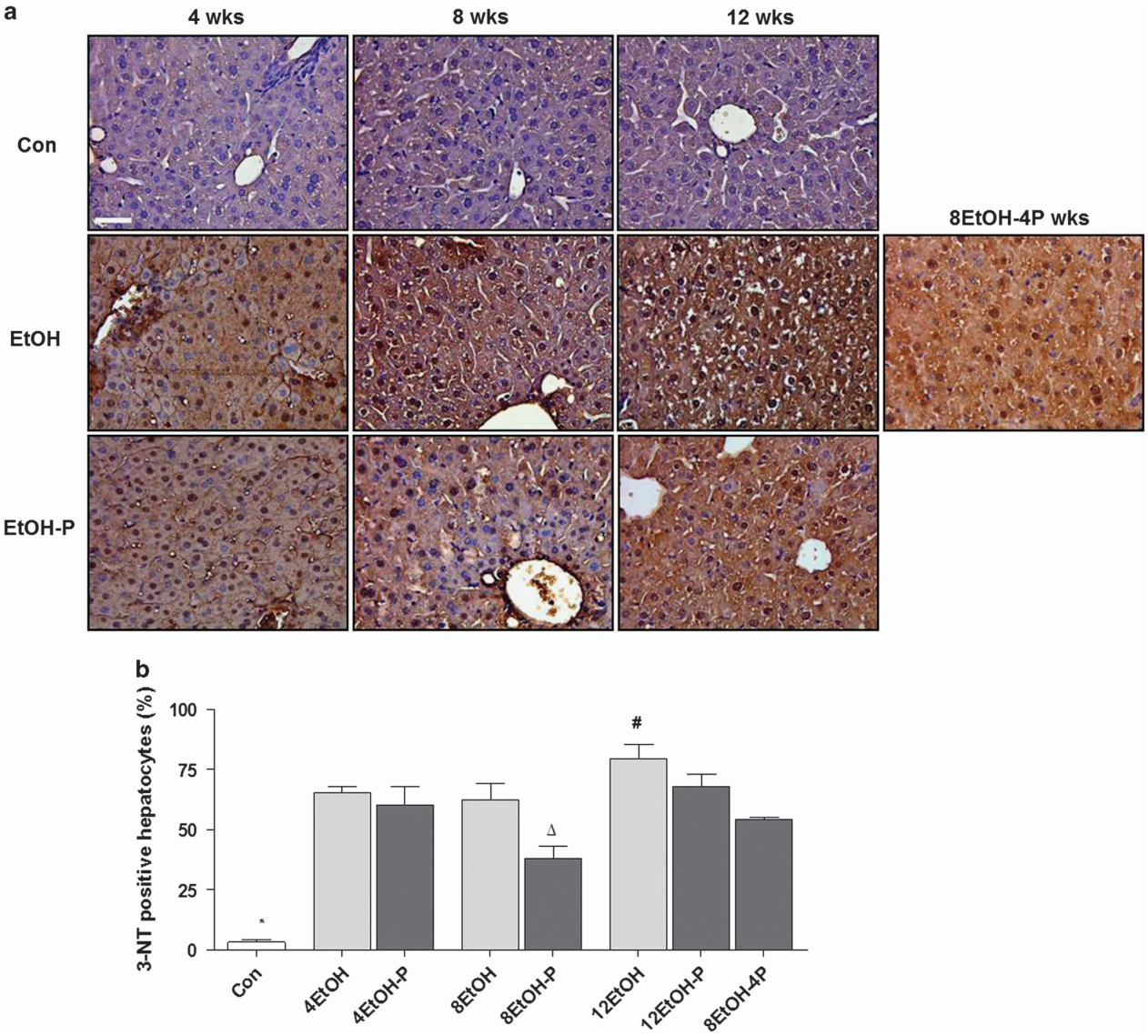


**Figure 5** Levels of nitrotyrosine-positive cells in liver sections. (**a**) Representative photomicrographs of 3-nitrotyrosine (3-NT) immunoreactivity. Alcohol intake induced oxidative stress and protein nitration, while simultaneous intake of alcohol and the probiotic for 8 weeks reduced this effect. Bar = 100 μm for all panels. (**b**) Histogram showing the percentages of hepatocytes positive to 3-NT in the various groups studied. The analysis was conducted in a blind manner (using coded slides with the observer not knowing the source of them). $^{*}P < 0.001$ vs. all other groups; $^{\Delta}P < 0.001$ vs. 4EtOH-P, 8EtOH, and 12EtOH-P; $^{\#}P < 0.05$ vs. 8EtOH, 8EtOH-4P. For the meaning of the abbreviations in **a** and **b**, indicating each mouse group, see legend for Figure 1 and Table 1. Con, control; 4EtOH, ethanol-fed mice for 4 weeks; 8EtOH, ethanol-fed mice for 8 weeks; 12EtOH, ethanol-fed mice for 12 weeks; 4EtOH-P, ethanol and probiotic-fed mice for 4 weeks; 8EtOH-P, ethanol and probiotic-fed mice for 8 weeks; 12EtOH-P, ethanol and probiotic-fed mice for 12 weeks; 8EtOH-4P, ethanol-fed mice for 8 weeks and then given probiotic for 4 weeks; wks, weeks.

microbiota, owing to its association with a wide range of diseases such as obesity, type 2 diabetes, inflammatory bowel disease, and the diseases caused by alcohol abuse.[50]

Our results show that, in mice, chronic alcohol feeding leads to a significant increase of liver steatosis classified as grade II in 8EtOH and grade III in 12EtOH. Counterparts fed with the probiotic showed a significant decrease of alcohol-induced liver steatosis from grade II and III to grade I. These findings are consistent with studies showing a correlation between dietary supplementation with probiotics and lipid metabolisms and reduction of fat accumulation in the liver.[51,52] Liver damage was marked at 12 weeks of EtOH administration and the probiotic had the capacity to protect against the pathogenic alcohol effects as indicated by a decrease in the levels of AST. Similarly, serum ALT levels were significantly higher at 12 weeks of EtOH administration compared with the other groups and, although there was a significant increase after 4 and 8 weeks, the reduction occurred only after a prolonged exposure to the probiotic.

Other authors have used mice to evaluate the effects of protein nitration in acute and chronic liver diseases.[53] In alcohol-exposed wild-type mice, the expression of iNOS was proportional to the levels of hepatic nitration and inhibition of mitochondrial function, whereas the *iNOS*( – / – ) mice showed

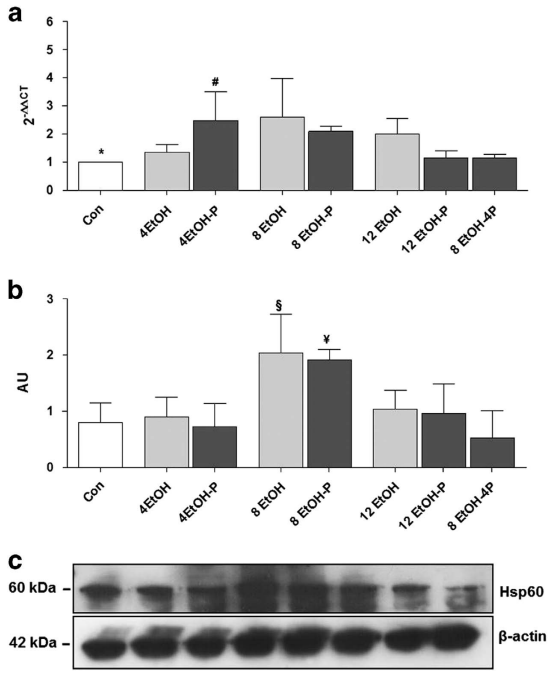


**Figure 6** *hsp60* gene expression and Hsp60 protein levels in the liver. (**a**) The bars show the levels of *hsp60* gene expression normalized for the reference genes, according to the Livak method ($2^{-\Delta\Delta CT}$), in the liver of control (Con), ethanol diets, and ethanol and probiotic diet mice. (**b**) Western blotting results. Ratio Hsp60 levels/β-actin levels as a reflection of Hsp60 increase (mean ± s.d.). (**c**) Representative cropped western blots for Hsp60 in control and ethanol-fed mice. All gels were run under the same experimental conditions and β-actin was used as an internal control. $^{*}P < 0.01$ vs. 4EtOH-P, 8EtOH; $^{\#}P < 0.05$ vs. 12EtOH-P; $^{\S}P < 0.05$ vs. Con and 4EtOH; $^{¥}P < 0.05$ vs. Con, 4EtOH-P. For the meaning of the abbreviations in **a** and **b**, indicating each mouse group, see legend for Figure 1 and Table 1. AU, arbitrary unit; Con, control; 4EtOH, ethanol-fed mice for 4 weeks; 8EtOH, ethanol-fed mice for 8 weeks; 12EtOH, ethanol-fed mice for 12 weeks; 4EtOH-P, ethanol and probiotic-fed mice for 4 weeks; 8EtOH-P, ethanol and probiotic-fed mice for 8 weeks; 12EtOH-P, ethanol and probiotic-fed mice for 12 weeks; 8EtOH-4P, ethanol-fed mice for 8 weeks and then given probiotic for 4 weeks; wks, weeks.

decreased levels of nitrated proteins and more resistance to alcoholic fatty liver disease.[54] Moreover, ethanol-induced production of NO via induction of iNOS increased the liver susceptibility to hypoxia and induced depression of mitochondrial energy state, leading to energy depletion and, ultimately, to the development of alcohol-mediated hepatic injury.[55] In our experiments, *iNOS* gene expression did not change after EtOH administration, which may be a reflection of post-transcriptional regulation of this enzyme. Western blotting showed that EtOH consumption increased iNOS levels in all EtOH-fed mouse groups in accordance with other studies in which levels of iNOS were increased following the exposure to EtOH.[56,57] The increase reached high levels after 8 and 12 weeks of EtOH administration, whereas a decrease of iNOS levels was observed in 12EtOH-P and in 8EtOH-4P compared with 12EtOH group. These data were confirmed by the analysis of the distribution of iNOS immunoreactivity. *L. fermentum* reduced significantly iNOS levels in the liver, confirming that this lactic acid bacterium has the capacity to decrease the toxic effect of alcohol as previously described.[58]

The combination of NO and superoxide produces peroxynitrite, which is known to be an important mediator in various pathological conditions, including liver diseases. Peroxynitrite can modify tyrosine (Tyr) residue(s) of many proteins in different cell compartments resulting in protein nitration, which alters their structure and function.[53] In our study, 3-NT immunoreactivity increased significantly in EtOH-fed mice and its distribution was both cytoplasmic and nuclear. It has been reported that protein nitration has an important role in promoting the ethanol-mediated mitochondrial dysfunction, hepatic toxicity, and intestinal barrier dysfunction.[59] *L. fermentum* reduced 3-NT levels in 8EtOH-P and in 8EtOH-4P compared with 8EtOH and 12EtOH, respectively. Moreover, in 8EtOH-P mice, 3-NT decreased significantly compared with all the probiotic-fed mouse groups. In this regard, relevant to our findings, it has been shown that *L. fermentum* has antioxidant properties in as much as it reduced lipid peroxidation and enhanced the antioxidant activity of glutathione peroxidase and glutathione reductase.[60–62]

As Hsps have a role in the protection of many cellular components during alcohol stress,[63] we focused on the mitochondrial chaperonin Hsp60 and its gene's expression levels by measuring mRNA as well as the levels of the gene's product by quantifying Hsp60 protein in liver tissue. The data showed that *hsp60* gene expression and the levels of Hsp60 protein levels were elevated in 8EtOH mouse group compared with the control group, and in 8EtOH-P compared with 4EtOH-P. Immunohistochemical staining revealed that Hsp60 immunoreactivity increased with the increase of alcohol intake, but it decreased after 12 weeks of alcohol consumption alone or in combination with the probiotic. Hsp60 increase in the liver of 8EtOH-fed mice may be considered as a protective mechanism against oxidative stress to maintain tissue homeostasis. After 12 weeks of ethanol administration, mitochondrial dysfunction likely leads to a reduction in *hsp60* gene expression and in the levels of Hsp60 protein. One of the cytoprotective effects of Hsps is related to their ability to inhibit apoptosis. Hsp60 forms a complex with procaspase-3 and displays an antiapoptotic effect.[64] In cardiac myocytes, Hsp60 has an antiapoptotic role by forming a macromolecular complex with Bax and Bak and, thereby, blocking their ability to induce apoptosis.[65] Thus, reduced levels of Hsp60 may exacerbate ALD as more Bax and Bak are released in response to alcohol-induced stress.[66] The increase of oxidative stress is due, in part, to impaired folding of the manganese superoxide dismutase, a key endogenous antioxidant enzyme. It has been demonstrated that Hsp60 and manganese superoxide dismutase proteins interact because manganese superoxide dismutase is a substrate of the Hsp60 folding machinery.[67] Hsp60 specifically associates with mitochondrial ATP synthase, the enzyme necessary to produce and hydrolyze ATP, protecting ATP synthase from degradation.[68] Therefore, Hsp60 participates in the maintenance of the balance between oxidants and antioxidants in ALD.

As stated above, protein nitration in chronic and acute liver diseases may result in structural and functional alterations of each target protein, as for example the loss of the catalytic activity if the target protein is an enzyme.[53] In our experiments, chronic EtOH intake significantly increased Hsp60 nitration,

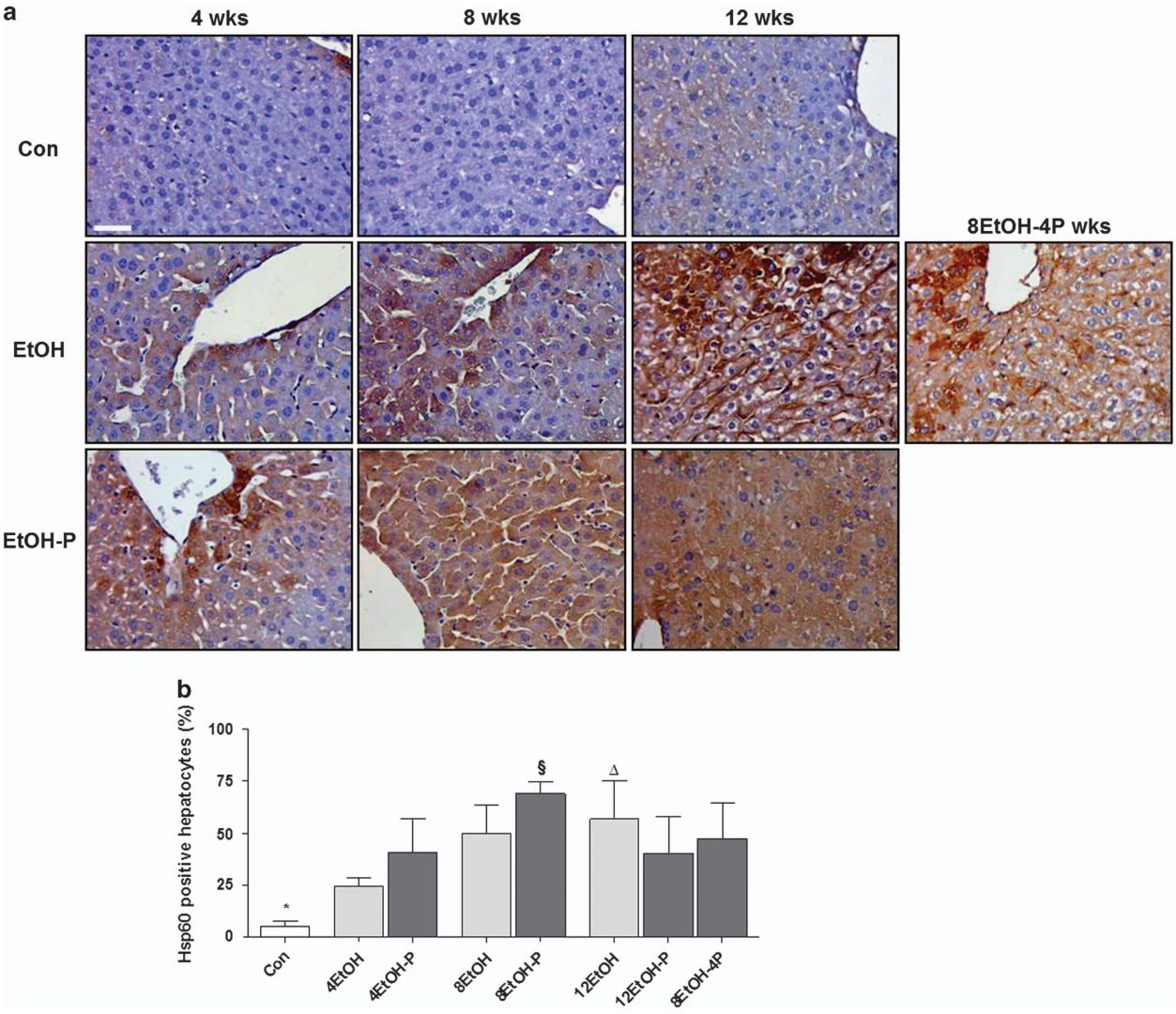


**Figure 7** Levels and preferential localization of Hsp60 in control and ethanol-fed mice. (**a**) Liver sections stained with a monoclonal antibody specific for Hp60. Bar = 100 μm for all panels. (**b**) Histogram showing the percentages of hepatocytes positive to Hsp60. The analysis was conducted in a blind manner (using coded slides with the observer not knowing the source of them). $^{*}P < 0.001$ vs. all other groups (except for 4EtOH); $^{\Delta}P < 0.001$ vs. 4EtOH; §$P < 0.05$ vs. 4EtOH-P and 12EtOH-P. For the meaning of the abbreviations in **a** and **b**, indicating each mouse group, see legend for Figure 1 and Table 1. Con, Control; 4EtOH, ethanol-fed mice for 4 weeks; 8EtOH, ethanol-fed mice for 8 weeks; 12EtOH, ethanol-fed mice for 12 weeks; 4EtOH-P, ethanol and probiotic-fed mice for 4 weeks; 8EtOH-P, ethanol and probiotic-fed mice for 8 weeks; 12EtOH-P, ethanol and probiotic-fed mice for 12 weeks; 8EtOH-4P, ethanol-fed mice for 8 weeks and then given probiotic for 4 weeks; wks, weeks.

and after 12 weeks of *L. fermentum* and EtOH consumption, Hsp60 nitration decreased, suggesting a protective role of the probiotic against nitrosative stress. Recent studies demonstrated that Hsp60 nitration in hyperglycemia not only causes a significant decrease in the ATP hydrolysis rate but also altered the interaction of the protein with its cochaperone Hsp10, impairing Hsp60 folding activity.[69] In fact, the nitration occurred in the hydrophobic position Y222 and Y226 in the apical domain of the chaperonin, a domain crucial for cochaperone and substrate binding of Hsp60.[14,69] Then, altered mitochondrial protein folding because of Hsp60/Hsp10 dysfunction or defective substrate binding could alter mitochondrial functionality, leading to the perpetuation of liver injury.

Therefore, our study showed that oral intake of *L. fermentum* protects against alcohol-induced liver injury in mice. The cellular and molecular mechanisms involved in this protection remain to be elucidated. ALD pathogenesis requires endotoxemia, and increased intestinal permeability is the major cause of endotoxemia. This gut leakiness is dependent on alcohol stimulation of iNOS in both alcoholic subjects and rodent models of alcoholic steatohepatitis. *L. fermentum* might cause the liver-protective effects by preventing endotoxemia by improving the intestinal barrier function like other strains do, and/or by enhancing the antioxidant activity of glutathione peroxidase and glutathione reductase.[60–62,70] The probiotic tested could decrease iNOS levels and ameliorate the inflammation because

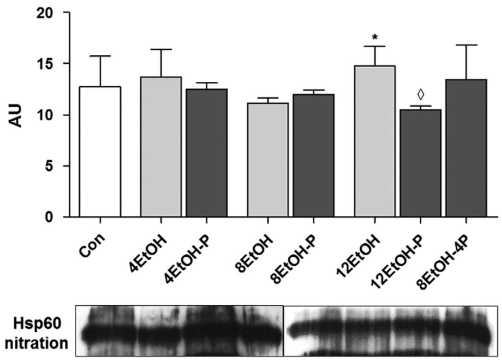


**Figure 8** Ethanol induced Hsp60 nitration. Representative western blots are shown below the densitometry histogram. $^{*}P<0.05$ vs. 8EtOH; $^{\lozenge}P<0.01$ vs. 12EtOH. For the meaning of the abbreviations indicating each mouse group, see legend for Figure 1 and Table 1. AU, arbitrary unit; Con, control; 4EtOH, ethanol-fed mice for 4 weeks; 8EtOH, ethanol-fed mice for 8 weeks; 12EtOH, ethanol-fed mice for 12 weeks; 4EtOH-P, ethanol and probiotic-fed mice for 4 weeks; 8EtOH-P, ethanol and probiotic-fed mice for 8 weeks; 12EtOH-P, ethanol and probiotic-fed mice for 12 weeks; 8EtOH-4P, ethanol-fed mice for 8 weeks and then given probiotic for 4 weeks; wks, weeks.

of its capacity to modulate nuclear factor-κB and tumor necrosis factor-α expression.[71,72] Also, *L. fermentum* administration in mice can induce significant shifts in the indigenous microbial community,[73] probably to a less toxic composition.

A major concern for the use of probiotics *in vivo* is that they must survive and sustain transit through the extreme conditions of the gastrointestinal tract in large quantities to allow their colonization in the host, and thus bring about the expected benefits. A solution to this problem may be achieved by developing encapsulation techniques to ensure greater survival of probiotic bacteria in the stomach and intestine. These techniques aim at protecting bacteria from detrimental factors such as high acidity (low pH) or bile salts.[74] However, one may assume that the probiotic tested has a gut-protective effect and, possibly, antisteatotic and antioxidant effects in the liver. Our results provide novel insights, especially regarding Hsp60, that may be taken into account while devising new approaches for treating liver diseases associated with alcohol consumption. These therapeutic strategies could be useful in developing countries, in which efficacious treatment of ethanol-related diseases will have a significant socioeconomic impact as it might go a long way to resolve an important health-related problem with a very simple and affordable approach.

Other mouse models have been used to study alcoholic liver injury but have limitations and disadvantages, such as a relatively high mouse mortality, the need of extensive medical care throughout the experiments and of a technically challenging surgery that is difficult to perform in most laboratories, and the induction of only a mild elevation of ALT and mild liver fibrotic changes.[75–78] We have standardized a mouse model (Table 1) different from other existing models in various ways, mainly alcohol feeding modality, and use of Hsp60 (a molecule that is central to vital cellular processes directly affected by ethanol) as a key biomarker and of a probiotic as a response monitor. This model is useful for studying liver disease induced by protracted intake of ethanol and for testing pertinent therapeutic agents, probiotics in particular. In our model, ethanol was administered without anesthesia using a noninvasive technique avoiding mouse mortality and the use of potentially harmful surgical techniques. These qualities ensure reproducibility and facilitate the use of the model also in other laboratories. From a pathological point of view, our model clearly reveals elevation in serum ALT and AST levels (two- and threefold at 12 weeks compared with the Con), liver steatosis (after 8 and 12 weeks of alcohol feeding), and in induction of oxidative and nitrosative stresses. Liver fibrotic changes and inflammation were not analyzed in depth and we did not carry out measurements of the pertinent indicators, such as inflammatory cytokines.

We have tested *L. fermentum* as response indicator and found that it produced clear benefits in as much as it reduced considerably ethanol-induced tissue damage and deleterious post-translational modifications of the chaperone Hsp60. Similarly, a variety of other agents and probiotics could be tested as well using this model, which can also be used for elucidating the cellular and molecular mechanisms underlying the favorable effects of *L. fermentum* and to investigate further the impact of Hsp60 nitration on disease progression. The same approach could be extended to other tissues, chaperones, and molecules affected by ethanol to understand how these cellular components and their alterations participate in ethanol-related disease, all of which will pave the way to the development of efficacious therapies for this widespread and devastating condition.

## CONFLICT OF INTEREST

**Guarantor of the article**: Francesco Cappello, MD.
**Specific author contributions**: A.M.G., R.B., and F.C. conceived the study and designed the experiments. A.M.G. wrote the manuscript. A.M.G., R.B., F.R., C.C.B., and G.D.P. performed experiments and analyzed data. F.M. and C.S. performed the animal tissue collection. VM performed the determination of AST and ALT levels. F.F., G.Z., E.C.de.M., A.J. L.M., and F.C. contributed to discussions and manuscript writing. G.T., V.D.F., M.C., and F.C. provided funding. All authors reviewed the manuscript and approved the final version submitted.
**Financial support**: This work was carried out using instruments provided by the Euro-Mediterranean Institute of Science and Technology, and funded with the Italian National Operational Programme for Research and Competitiveness 2007–2013 grant awarded to the project titled "Cyber Brain—Polo di innovazione" (Project code: PONa3_00210, European Regional Development Fund). A.J.L.M. and E.C.de.M. were partially supported by IMET; A.J.L.M. and F.C. were partially supported by IEMEST. This work was carried out under the umbrella of the agreement between the Euro-Mediterranean Institute of Science and Technology (Italy) and Institute of Marine and Environmental Technology (USA) signed in March 2012 (this is IMET contribution number IMET 16-171).
**Potential competing interests**: None.

## Study Highlights

### WHAT IS CURRENT KNOWLEDGE

- ✓ Alcohol abuse leads to alcoholic liver disease (ALD).
- ✓ Oxidative/nitrosative stress are identified as key elements in the pathophysiology of ALD.
- ✓ Probiotics have antioxidant effects and are considered as a promising therapeutic strategy for steatohepatitis.

### WHAT IS NEW HERE

- ✓ A mouse model to study liver pathology caused by chronic ethanol intake that differs from existing ones in various ways, e.g., ethanol administration modality and inclusion of Hsp60 as a key indicator and of a probiotic as a response monitor. The model is fully characterized and designed to provide information on key disease indicators and to assess the curative efficacy of probiotics and other agents with therapeutic potential.
- ✓ The probiotic *L. fermentum* ameliorated key disease indicators and, as such, is also part of the model system to be used as a positive control and as a baseline for comparing beneficial effects when other probiotics or drugs are evaluated.


1. Mills SJ, Harrison SH. Comparison of the natural history of alcoholic and nonalcoholic fatty liver disease. *Curr Gastroenterol Rep* 2010; **7**: 32–36.
2. Stewart S, Jones D, Day CP. Alcoholic liver disease: new insights into mechanisms and preventative strategies. *Trends Mol Med* 2001; **7**: 408–413.
3. Arteel GE. Alcohol-induced oxidative stress in the liver: *in vivo* measurements. *Meth Mol Biol* 2008; **447**: 185–197.
4. Ambade A, Mandrekar P. Oxidative stress and inflammation: essential partners in alcoholic liver disease. *Int J Hepatol* 2012; **2012**: 853175.
5. Fransen M, Nordgren M, Wang B *et al.* Role of peroxisomes in ROS/RNS-metabolism: implications for human disease. *Biochim Biophys Acta* 2012; **1822**: 1363–1373.
6. Degli Esposti D, Hamelin J, Bosselut N *et al.* Mitochondrial roles and cytoprotection in chronic liver injury. *Biochem Res Int* 2012; **2012**: 387626.
7. Loguercio C, Federico A. Oxidative stress in viral and alcoholic hepatitis. *Free Radic Biol Med* 2003; **34**: 1–10.
8. Suciu M. The role of nitric oxide (NO) and statins in endothelial dysfunction and atherosclerosis. *Farmacia* 2009; **57**: 131–138.
9. Pacher P, Beckman J, Liaudet A. Nitric oxide and peroxynitrite in health and disease. *Physiol Rev* 2007; **87**: 315–424.
10. Radi R. Nitric oxide, oxidants and protein tyrosine nitration. *Proc Natl Acad Sci USA* 2004; **101**: 4003–4008.
11. Murata M, Kawanishi S. Oxidative DNA damage induced by nitrotyrosine: a biomarker of inflammation. *Biochem Biophys Res Commun* 2004; **316**: 123–128.
12. Finkel T, Holbrook NJ. Oxidants, oxidative stress and the biology of ageing. *Nature* 2000; **408**: 239–247.
13. Macario AJL, Conway de Macario E, Cappello F. *The Chaperonopathies. Diseases with Defective Molecular Chaperones.* Springer: Dordrecht-Heidelberg–New York–London. 2013.
14. Cappello F, Marino Gammazza A, Palumbo Piccionello A *et al.* Hsp60 chaperonopathies and chaperonotherapy: targets and agents. *Expert Opin Ther Targets* 2014; **18**: 185–208.
15. Vilasi S, Carrotta R, Mangione MR *et al.* Human Hsp60 with its mitochondrial import signal occurs in solution as heptamers and tetradecamers remarkably stable over a wide range of concentrations. *PLoS One* 2014; **9**: e97657.
16. Sarangi U, Singh MK, Abhijnya KV *et al.* Hsp60 chaperonin acts as barrier to pharmacologically induced oxidative stress mediated apoptosis in tumor cells with differential stress response. *Drug Target Insights* 2013; **7**: 35–51.
17. Campanella C, Bucchieri F, Merendino AM *et al.* The Odyssey of Hsp60 from tumor cells to other destinations includes plasma membrane-associated stages and Golgi and exosomal protein-trafficking modalities. *PLoS One* 2012; **7**: e42008.
18. Rakonczay Z Jr, Boros I, Jármay K *et al.* Ethanol administration generates oxidative stress in the pancreas and liver, but fails to induce heat-shock proteins in rats. *J Gastroenterol Hepatol* 2003; **18**: 858–867.
19. Arteel GE. Oxidants and antioxidants in alcohol-induced liver disease. *Gastroenterology* 2003; **124**: 778–790.
20. Shinde A, Ganu J, Naik P *et al.* Oxidative stress and antioxidative status in patients with alcoholic liver disease. *Biomed Res* 2012; **23**: 105–108.
21. Macaluso F, Barone R, Catanese P *et al.* Do fat supplements increase physical performance? *Nutrients* 2013; **5**: 509–524.
22. Bjelakovic G, Nikolova D, Simonetti RG *et al.* Antioxidant supplements for preventing gastrointestinal cancers. *Cochrane Database Syst Rev* 2008: CD004183.
23. Soccol CR, Porto de Souza Vandenberghe L, Spier MR *et al.* The potential of probiotics: a review. *Food Technol Biotechnol* 2010; **48**: 413–434.
24. Gionchetti P, Rizzello F, Venturi A *et al.* Oral bacteriotherapy as maintenance treatment in patients with chronic pouchitis: A double-blind, placebo-controlled trial. *Gastroenterology* 2000; **119**: 305–309.
25. Pronio A, Montesani C, Butteroni C *et al.* Probiotic administration in patients with ileal pouch-anal anastomosis for ulcerative colitis is associated with expansion of mucosal regulatory cells. *Inflamm Bowel Dis* 2008; **14**: 662–668.
26. Bellavia M, Tomasello G, Romeo M *et al.* Gut microbiota imbalance and chaperoning system malfunction are central to ulcerative colitis pathogenesis and can be counteracted with specifically designed probiotics: a working hypothesis. *Med Microbiol Immunol* 2013; **202**: 393–406.
27. Vilela EG, De Lourdes de Abreu Ferrari M, Da Gama Torres HO *et al.* Influence of *Saccharomyces boulardii* on the intestinal permeability of patients with Crohn's disease in remission. *Scand J Gastroenterol* 2008; **43**: 842–848.
28. Stancu CS, Sanda GM, Deleanu M *et al.* Probiotics determine hypolipidemic and antioxidant effects in hyperlipidemic hamsters. *Mol Nutr Food Res* 2014; **58**: 559–568.
29. Canesso MCC, Lacerda NL, Ferreira CM *et al.* Comparing the effects of acute alcohol consumption in germ-free and conventional mice: the role of the gut microbiota. *BMC Microbiol* 2014; **14**: 240.
30. Carr RM, Peralta G, Yin X *et al.* Absence of perilipin 2 prevents hepatic steatosis, glucose intolerance and ceramide accumulation in alcohol-fed mice. *PLoS One* 2014; **9**: e97118.
31. Carr RM, Dhir R, Yin X *et al.* Temporal effects of ethanol consumption on energy homeostasis, hepatic steatosis, and insulin sensitivity in mice. *Alcohol Clin Exp Res* 2013; **37**: 1091–1099.
32. Salamone F, Galvano F, Marino Gammazza A *et al.* Silibinin improves hepatic and myocardial injury in mice with nonalcoholic steatohepatitis. *Dig Liver Dis* 2012; **44**: 334–342.
33. Rappa F, Greco A, Podrini C *et al.* Immunopositivity for histone macroH2A1 isoforms marks steatosis-associated hepatocellular carcinoma. *PLoS One* 2013; **8**: e54458.
34. Sherlock S. Alcoholic liver disease. *Lancet* 1995; **345**: 227–229.
35. Barone R, Macaluso F, Catanese P *et al.* Endurance exercise and conjugated linoleic acid (CLA) supplementation up-regulate CYP17A1 and stimulate testosterone biosynthesis. *PLoS One* 2013; **8**: e79686.
36. Di Felice V, Serradifalco C, Rizzuto L *et al.* Silk fibroin scaffolds enhance cell commitment of adult rat cardiac progenitor cells. *J Tissue Eng Regen Med* 2015; **9**: E51–E64.
37. Livak KJ, Schmittgen TD. Analysis of relative gene expression data using real-time quantitative PCR and the 2( – Delta Delta C(T)) Method. *Methods* 2001; **25**: 402–408.
38. Orban G, Bombardi C, Marino Gammazza A *et al.* Role(s) of the 5-HT2C receptor in the development of maximal dentate activation in the hippocampus of anesthetized rats. *CNS Neurosci Ther* 2014; **20**: 651–661.
39. Marino Gammazza A, Rizzo M, Citarrella R *et al.* Elevated blood Hsp60, its structural similarities and cross-reactivity with thyroid molecules, and its presence on the plasma membrane of oncocytes point to the chaperonin as an immunopathogenic factor in Hashimoto's thyroiditis. *Cell Stress Chaperones* 2014; **19**: 343–353.
40. Rappa F, Sciume C, Lo Bello M *et al.* Comparative analysis of Hsp10 and Hsp90 expression in healthy mucosa and adenocarcinoma of the large bowel. *Anticancer Res* 2014; **34**: 4153–4159.
41. Szabo G, Bala S. Alcoholic liver disease and the gut-liver axis. *World J Gastroenterol* 2010; **16**: 1321–1329.
42. Bode C, Bode JC. Effect of alcohol consumption on the gut. *Best Pract Res Clin Gastroenterol* 2003; **17**: 575–592.
43. Duerkop BA, Vaishnava S, Hooper LV. Immune responses to the microbiota at the intestinal mucosal surface. *Immunity* 2009;**31**:368–376.
44. Mutlu E, Keshavarzian A, Engen P *et al.* Intestinal dysbiosis: a possible mechanism of alcohol-induced endotoxemia and alcoholic steatohepatitis in rats. *Alcohol Clin Exp Res* 2009; **33**: 1836–1846.
45. Basuroy S, Sheth P, Mansbach CM *et al.* Acetaldehyde disrupts tight junctions and adherens junctions in human colonic mucosa: protection by EGF and L-glutamine. *Am J Physiol Gastrointest Liver Physiol* 2005; **289**: G367–G375.
46. Wang L, Song Z, Lambert JC *et al.* A critical involvement of oxidative stress in acute alcohol-induced hepatic TNF-alpha production. *Am J Pathol* 2003; **163**: 1137–1146.
47. Banan A, Fields JZ, Decker H *et al.* Nitric oxide and its metabolites mediate ethanol-induced microtubule disruption and intestinal barrier dysfunction. *J Pharmacol Exp Ther* 2000; **294**: 997–1008.
48. Tang Y, Banan A, Forsyth CB *et al.* Effect of alcohol on miR-212 expression in intestinal epithelial cells and its potential role in alcoholic liver disease. *Alcohol Clin Exp Res* 2008; **32**: 355–364.
49. Bull-Otterson L, Feng W, Kirpich I *et al.* Metagenomic analyses of alcohol induced pathogenic alterations in the intestinal microbiome and the effect of *Lactobacillus rhamnosus* GG treatment. *PLoS One* 2013; **8**: e53028.
50. Nguyen TL, Vieira-Silva S, Liston A *et al.* How informative is the mouse for human gut microbiota research? *Dis Model Mech* 2015; **8**: 1–16.

51. Paik HD, Park JS, Park E. Effects of *Bacillus polyfermenticus* SCD on lipid and antioxidant metabolisms in rats fed a high-fat and high-cholesterol diet. *Biol Pharm Bull* 2005; **28**: 1270–1274.
52. Li C, Nie SP, Zhu KX *et al. Lactobacillus plantarum* NCU116 improves liver function, oxidative stress and lipid metabolism in rats with high fat diet induced non-alcoholic fatty liver disease. *Food Funct* 2014; **5**: 3216–3223.
53. Abdelmegeed MA, Song BJ. Functional roles of protein nitration in acute and chronic liver diseases. *Oxid Med Cell Longev* 2014; **2014**: 149627.
54. McKim SE, Gabele E, Isayama F *et al.* Inducible nitric oxide synthase is required in alcohol-induced liver injury: studies with knockout mice. *Gastroenterology* 2003; **125**: 1834–1844.
55. Zelickson BR, Benavides GA, Johnson MS *et al.* Nitric oxide and hypoxia exacerbate alcohol-induced mitochondrial dysfunction in hepatocytes. *Biochim Biophys Acta* 2011; **1807**: 1573–1582.
56. Venkatraman A, Shiva S, Wigley A *et al.* The role of iNOS in alcohol-dependent hepatotoxicity and mitochondrial dysfunction in mice. *Hepatology* 2004; **40**: 565–573.
57. Moon KH, Hood BL, Kim BJ *et al.* Inactivation of oxidized and S-nitrosylated mitochondrial proteins in alcoholic fatty liver of rats. *Hepatology* 2006; **44**: 1218–1230.
58. Kim Ji-Hyun, Kim Hyun-Jin, Jeong Hwa Son *et al.* Effect of *Lactobacillus fermentum* MG590 on alcohol metabolism and liver function in rats. *J Microbiol Biotechnol* 2003; **13**: 919–925.
59. Keshavarzian A, Holmes EW, Patel M *et al.* Leaky gut in alcoholic cirrhosis: a possible mechanism for alcohol-induced liver damage. *Am J Gastroenterol* 1999; **94**: 200–207.
60. Sharma R, Kapila R, Kapasiya M *et al.* Dietary supplementation of milk fermented with probiotic *Lactobacillus fermentum* enhances systemic immune response and antioxidant capacity in aging mice. *Nutr Res* 2014; **34**: 968–981.
61. Persichetti E, De Michele A, Codini M *et al.* Antioxidative capacity of *Lactobacillus fermentum* LF31 evaluated *in vitro* by oxygen radical absorbance capacity assay. *Nutrition* 2014; **30**: 936–938.
62. Kullisaar T, Songisepp E, Aunapuu M *et al.* Complete glutathione system in probiotic *Lactobacillus fermentum* ME-3. *Prikl Biokhim Mikrobiol* 2010; **46**: 527–531.
63. Tóth ME, Vígh L, Sántha M. Alcohol stress, membranes, and chaperones. *Cell Stress Chaperones* 2014; **19**: 299–309.
64. Campanella C, Bucchieri F, Ardizzone NM *et al.* Upon oxidative stress, the antiapoptotic Hsp60/procaspase-3 complex persists in mucoepidermoid carcinoma cells. *Eur J Histochem* 2008; **52**: 221–228.
65. Kirchhoff SR, Gupta S, Knowlton AA. Cytosolic heat shock protein 60, apoptosis, and myocardial injury. *Circulation* 2002; **105**: 2899–2904.
66. Dufour J, Clavien P. *Signaling Pathways in Liver Diseases. Springer Science*, 2nd edn Springer: New York, NY, USA, 2009.
67. Magnoni R, Palmfeldt J, Hansen J *et al.* The Hsp60 folding machinery is crucial for manganese superoxide dismutase folding and function. *Free Radic Res* 2014; **48**: 168–179.
68. Alard JE, Hillion S, Guillevin L *et al.* Autoantibodies to endothelial cell surface ATP synthase, the endogenous receptor for hsp60, might play a pathogenic role in vasculatides. *PLoS One* 2011; **6**: e14654.
69. Koeck T, Corbett JA, Crabb JW *et al.* Glucose-modulated tyrosine nitration in beta cells: targets and consequences. *Arch Biochem Biophys* 2009; **484**: 221–231.
70. Forsyth CB, Farhadi A, Jakate SM *et al. Lactobacillus* GG treatment ameliorates alcohol-induced intestinal oxidative stress, gut leakiness, and liver injury in a rat model of alcoholic steatohepatitis. *Alcohol* 2009; **43**: 163–172.
71. Frick JS, Schenk K, Quitadamo M *et al. Lactobacillus fermentum* attenuates the proinflammatory effect of *Yersinia enterocolitica* on human epithelial cells. *Inflamm Bowel Dis* 2007; **13**: 83–90.
72. Hegazy SK, El-Bedewy MM. Effect of probiotics on pro-inflammatory cytokines and NF-kappaB activation in ulcerative colitis. *World J Gastroenterol* 2010; **16**: 4145–4151.
73. Lam C, Conway PL, O'Riordan K. Gastrointestinal microbial community shifts observed following oral administration of a *Lactobacillus fermentum* strain to mice. *FEMS Microbiol Ecol* 2003; **43**: 133–140.
74. Arora S, Kaur IP, Chopra K *et al.* Efficiency of double layered microencapsulated probiotic to modulate proinflammatory molecular markers for the management of alcoholic liver disease. *Mediators Inflamm* 2014;**2014**:715130.
75. de la M, Hall P, Lieber CS *et al.* Models of alcoholic liver disease in rodents: a critical evaluation. *Alcohol Clin Exp Res* 2001;**25**:254–261.
76. Deng QG, She H, Cheng JH *et al.* Steatohepatitis induced by intragastric overfeeding in mice. *Hepatology* 2005; **42**: 905–914.
77. Bouchard JC, Kim J, Beal DR *et al.* Acute oral ethanol exposure triggers asthma in cockroach allergen-sensitized mice. *Am J Pathol* 2012; **181**: 845–857.
78. Williams JA, Manley S, Ding WX. New advances in molecular mechanisms and emerging therapeutic targets in alcoholic liver diseases. *World J Gastroenterol* 2014; **20**: 12908–12933.

***Clinical and Translational Gastroenterology*** **is an open-access journal published by** ***Nature Publishing Group*****. This work is licensed under a Creative Commons Attribution-NonCommercial-NoDerivs 4.0 International License. The images or other third party material in this article are included in the article's Creative Commons license, unless indicated otherwise in the credit line; if the material is not included under the Creative Commons license, users will need to obtain permission from the license holder to reproduce the material. To view a copy of this license, visit http://creativecommons.org/licenses/by-nc-nd/4.0/**

Supplementary Information accompanies this paper on the Clinical and Translational Gastroenterology website (http://www.nature.com/ctg)